Continuous-Curvature Paths for Autonomous Vehicles

Winston Nelson

AT&T Bell Laboratories
Murray Hill, New Jersey 07974

ABSTRACT

The paths followed by autonomously guided vehicles (AGVs) are generally made up of line and circular-arc segments. For most AGVs, the steering functions required to keep the position and heading of the cart continuously aligned with such paths have discontinuities at the line-arc-line transition points, because the curvature of the path is discontinuous at these points. For applications where continuous-curvature paths are desired, two types of curves are proposed: (1) polar polynomials in place of circular-arc segments, and (2) cartesian polynomials in place of arc-arc or arc-line-arc segments for lane-change maneuvers. Both curves have computationally simple, closed-form expressions that provide continuous curvature and precise matching of the the boundary conditions at the line-curve junctions on the paths. The use of these curves in place of circular arcs for the reference path generator on an experimental AGV has improved its tracking accuracy during and following turns, particularly at higher speeds.

1. INTRODUCTION

The paths for routing autonomously guided vehicles (AGVs) around factories or offices generally comprise a concatenation of line and circular-arc segments. For most AGVs, the steering functions required to keep the position and heading of the cart continuously aligned with such paths have discontinuities at the line-arc-line transition points, because the curvature of the path is discontinuous at these points. Since instantaneous changes in steering mechanisms are physically impossible, errors in position and heading of the AGV will result at each junction of line and circular-arc segments. Proper feedback control design can reduce these errors to transient errors which disappear, hopefully, before reaching locations on the path where highly accurate positioning of the AGV is required. However, even if such control is achieved, the rapid changes in steering required to achieve rapid error recovery may violate dynamic constraints on the AGV or its cargo. Reducing the path velocity[1], [2], can correct this problem, but only at the expense of overall AGV task-efficiency. Another means of avoiding steering discontinuities is to move the guide point (i.e., the point on the AGV that is tracking the path) away from the AGV center-of-rotation point. This permits the position of the AGV to follow a line-circular-arc path with a continuous steering function[2],[3]. However, the heading of the cart remains mis-aligned with the path for a considerable distance after the circular-arc turn[3].

This paper discusses eliminating steering discontinuity problems by replacing the circular-arc segments with curve segments that provide continuous-curvature paths without any significant increase in the computational complexity in generating such paths.

2. CONTINUOUS-CURVATURE PATHS

While arcs of circles are geometrically convenient for the curved portions of paths, and in some cases are optimal for constructing minimum length paths[4], they are not the only type of curve which should be considered in generating paths for robot carts. Since circular arcs have constant curvature equal to the inverse of the radius, R, of the circle, and lines have zero curvature, discontinuities in curvature of magnitude $1/R$ occur at every junction point between the lines and circular arcs on the path. As discussed above, this results in discontinuities in the steering functions required to keep the AGV position and heading aligned with the path. A continuous curvature path is clearly one in which all the curve segments have continuous curvature within their segment length and zero curvature at their end-point junctions with the line segments.

One type of curve which has been used for continuous-curvature path generation is a "clothoid" curve segment. A clothoid or Cornu spiral[5] is a curve whose curvature is a linear function of distance along the curve. Kanayama and Miyake[6] use a "clothoid pair" to make curves with zero curvature at their junctures with line segments, in order to produce continuous drive-velocity functions for a differential-drive cart. Clothoid pairs have the advantage of providing the minimum-length curves for a given limit on jerk (see Appendix); they have the disadvantage, however, that the (x,y) coordinates of the curve have no closed-form expressions, but must be derived by integrating along the path length, s, with the curvature, $\kappa(s)$ linearly increasing from zero during the first half of the turn, then linearly decreasing to zero during the second half, in such a way that the end-point of the curve precisely matches the position and slope constraints of the succeeding line segment. Any errors in the slope of the curvature function, or in the numerical integration routine may result in mis-match of these end-point conditions.

A second type of continuous-curvature curve is the "cubic spiral", proposed by Kanayama and Hartman[7]. It provides an optimally smooth path for turns, in the sense of minimizing the integral-square-jerk on a vehicle moving through the turn at constant speed (see Appendix). While somewhat simpler to generate than the clothoid-pair, it shares its disadvantage of lacking a closed-form expression for the curve coordinates.

In this section we describe as alternatives to clothoid pairs, cubic spirals, or other path-length functions, two types of continuous-curvature polynomial functions -- one for arc turns and one for lane changes. Both types have closed-form expressions that match *a priori* the boundary conditions of the two lines they join[8].

CH2750-8/89/0000/1260$01.00 © 1989 IEEE

2.1 Arc Turns

Curves that produce a smooth transition between lines intersecting at an arbitrary turn angle, and are symmetric with respect to the line bisecting the angle, will be called "arc turns". The turn angle, Θ, is measured in the direction of the change of heading, with counter-clockwise positive. We assume that a circular arc of radius, R, has been given by the path planner as an initial realization of the arc turn.

To obtain a curve that does not deviate too far in shape from the circular arc it will replace, and yet satisfies the position, heading, and curvature constraints imposed at the start and end points, the coordinates of the curve should be chosen so that the independent variable changes relatively uniformly with respect to the distance along the curve, regardless of the total angle. It seems appropriate, therefore, to consider polar coordinates, with the curve specified by the polar radial, r, as a polynomial function of the polar angle, ϕ, with the general form,

$$r(\phi) = a_0+a_1\phi+a_2\phi^2+a_3\phi^3+a_4\phi^4+ \cdots \quad , \tag{1}$$

where the number of terms needed depends on the number of conditions imposed.

Consider arc turns transformed into the coordinate frame shown in Figure 1. For the desired continuous-curvature replacement for the circular arc, the position, slope, and curvature constraints on the polynomial (1) are:

$$\begin{aligned} &r=R \ , \quad r'=0 \ , \quad \kappa=0 \quad \text{at} \quad \phi=0 \ , \\ &r=R \ , \quad r'=0 \ , \quad \kappa=0 \quad \text{at} \quad \phi=\Theta \ , \end{aligned} \tag{2}$$

where $r' \equiv dr/d\phi$ and κ is the curvature of r. The general expression for curvature of any curve is

$$\kappa = d\theta/ds \quad , \tag{3}$$

where s is the path-length variable and θ is the angle of the tangent to the path (also the *heading* of a vehicle whose center of rotation is following the path[3]).

For a path defined in polar coordinates (r,ϕ), the tangent angle can be expressed as

$$\theta = \pi/2 + \phi - \tan^{-1}(r'/r) \quad . \tag{4}$$

Differentiating (4) with respect to ϕ gives

$$\frac{d\theta}{d\phi} = 1 - \frac{rr'' - r'^2}{r^2 + r'^2} \quad , \tag{5}$$

where $r'' \equiv d^2r/d\phi^2$.

The infinitesimal change in path length, ds, is given in polar form by

$$ds = (r^2 + r'^2)^{1/2} d\phi \quad . \tag{6}$$

Using (5) and (6) in (3) yields the desired expression for the curvature, namely:

$$\kappa = \frac{r^2 + 2r'^2 - rr''}{(r^2 + r'^2)^{3/2}} \quad . \tag{7}$$

Using the position and slope constraints of (2) in (7), it follows that the zero curvature constraints in (2) are equivalent to requiring that $r''=R$ at $\phi=0$ and $\phi=\Theta$. Applying these constraints on r, r', and r'' yields four non-zero coefficients in (1), namely: $a_0=R$, $a_2=R/2$, $a_3=-R/\Theta$, and $a_4=R/2\Theta^2$. The single polar-polynomial (SPP) curve for the desired fit between line segments can thus be written as

$$r(\phi) = R\left[1 + \frac{\phi^2}{2} - \frac{\phi^3}{\Theta} + \frac{\phi^4}{2\Theta^2}\right] \quad . \tag{8}$$

The (x,y) coordinates of the SPP curve are given by $x=r\cos\phi$ and $y=r\sin\phi$. These coordinates and the heading (4) are then converted back to the original path coordinates by the inverse of the transformation used to convert from the path to the coordinate frame shown in Figure 1.

The continuous-curvature SPP curves resulting from (8) are shown in Figure 1 for four values of the turn angle, Θ, and $R=1$.

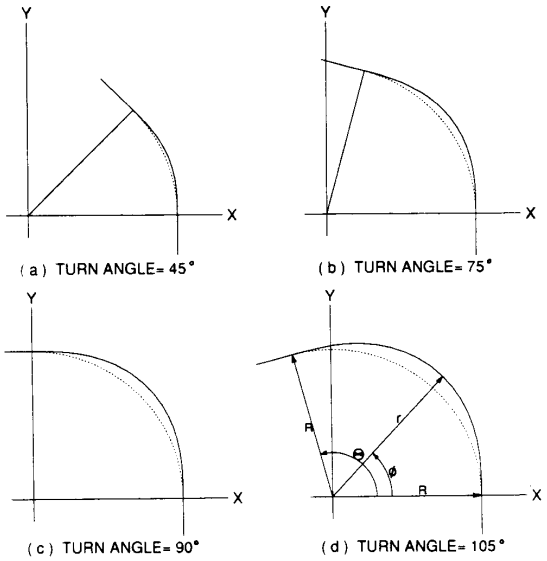

Fig. 1. Single polar polynomial(SPP) curves for unit radius arc turns. The corresponding circular arcs for R=1 are shown as dotted lines.

The curvature functions, given by (7), for these four SPP curves are plotted in Figure 2. The paths and curvatures for the corresponding circular arc turns are also shown in these figures. It

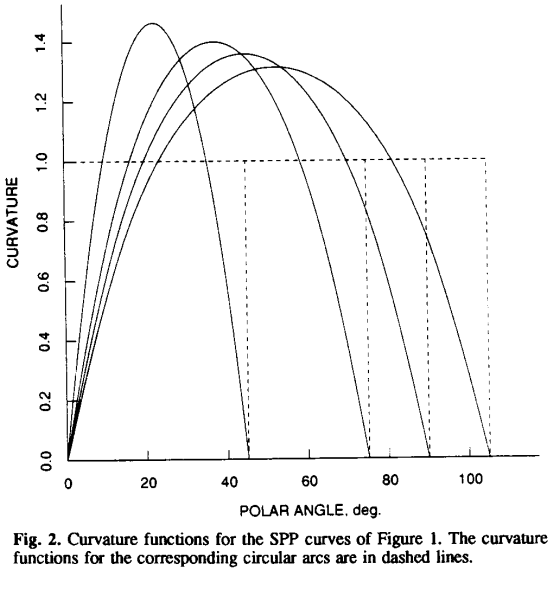

Fig. 2. Curvature functions for the SPP curves of Figure 1. The curvature functions for the corresponding circular arcs are in dashed lines.

is clear from the results shown in Figures 1 and 2 that the SPP curve is a suitable choice for producing continuous-curvature arc turns of arbitrary angle. It has a closed-form expression (8) which is a simple function of the turn radius, R, and turn angle, Θ. The curve it produces is symmetric and is reasonably close to the circular arc, although the separation between the two increases with turn angle. The curvature of SPP curves for arc turns of 90 degrees or less is very close to the parabolic shape of the curvature function for cubic spirals[7], as illustrated in Figure 3. This means that for such arc turns, SPP curves provide near-optimally smooth turns, in the minimum integral-square-jerk sense (see Appendix).

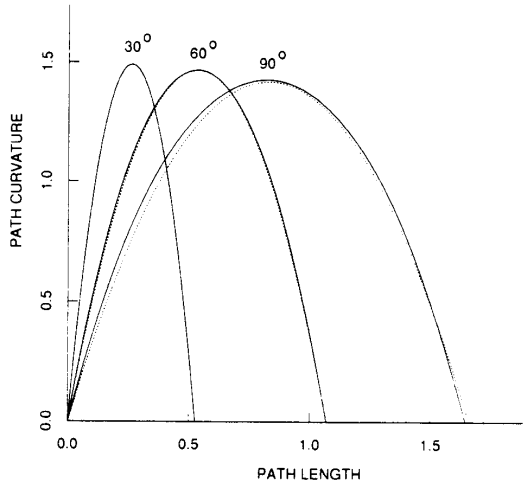

Fig. 3. Curvature as a function of path length for SPP curves (solid) and cubic spirals (dotted) for unit radius arc turns of 30, 60, and 90 degrees.

For arc turns of 90 degrees or more, if the deviation of the SPP curve from the circular-arc radius is too large for certain path-planning situations, the SPP curve (8) can be replaced with a piecewise polynomial function, or spline[9], consisting of two polar-polynomial segments separated by a circular-arc segment. Such polar splines can provide continuous-curvature arc turns that are closer to the circular arc than the single SPP curve, but at the expense of higher peak curvature and curvature rate.

Given a circular arc turn of angle Θ and radius R between two line segments, we construct a polar spline made up of three segments: a polar polynomial of the form given in (1) from ϕ=0 to ϕ=β, a circular arc of radius $R_b > R$ from ϕ=β to ϕ=Θ–β, and a polar polynomial from ϕ=Θ–β to ϕ=Θ. The position, slope, and curvature constraints on the polynomial (1) for the first segment are

$$\begin{aligned} r&=R\ , \quad r'=0\ , \quad \kappa=0 \qquad \text{at } \phi=0\ , \\ r&=R_b\ , \quad r'=0\ , \quad \kappa=1/R_b \quad \text{at } \phi=\beta\ , \end{aligned} \tag{9}$$

where $r' \equiv dr/d\phi$ and κ is the curvature of r. Following the procedure outlined above for the SPP, the first segment of the polar spline, satisfying the boundary constraints (9), is given by

$$r(\phi) = R\left[1 + \frac{\phi^2}{2} - \frac{\phi^3}{2\beta} + \frac{\phi^5}{10\beta^3}\right]\ , \tag{10}$$

where the break angle β (in radians) and radius R_b are constrained to satisfy

$$\beta^2 = 10\left(\frac{R_b}{R} - 1\right)\ , \quad R_b > R \tag{11}$$

The second segment of the polar spline is an arc of constant radius R_b, while the third segment is obtained from (10) by substituting Θ–ϕ in place of ϕ.

The constraint (11) was chosen to give a good compromise between the initial and final curvature slope (jerk) for the first and third segments. Note from (11) that the closer R_b is to R, the smaller must be the angle β. However, a smaller β produces a curve with larger peak curvature and curvature rate. Hence kinematic and dynamic constraints on the vehicle will generally set a lower bound on the break angle β and radius R_b. Figure 4(a) shows the polar spline (solid) for a 180-degree turn, compared to a circular arc (dotted) and SPP curve (dashed). The break angle, β=0.9 radians (51.6 deg.), chosen for this polar spline yields from (11) a radius R_b only 8% greater than the circular arc, compared to the 31% radial increase at the mid-point of the SPP curve. The curvature functions of these curves, shown in Figure 4(b), show that while the polar spline (solid) has a continuous curvature, it has greater peak curvature and peak curvature-rate than the SPP curve (dashed).

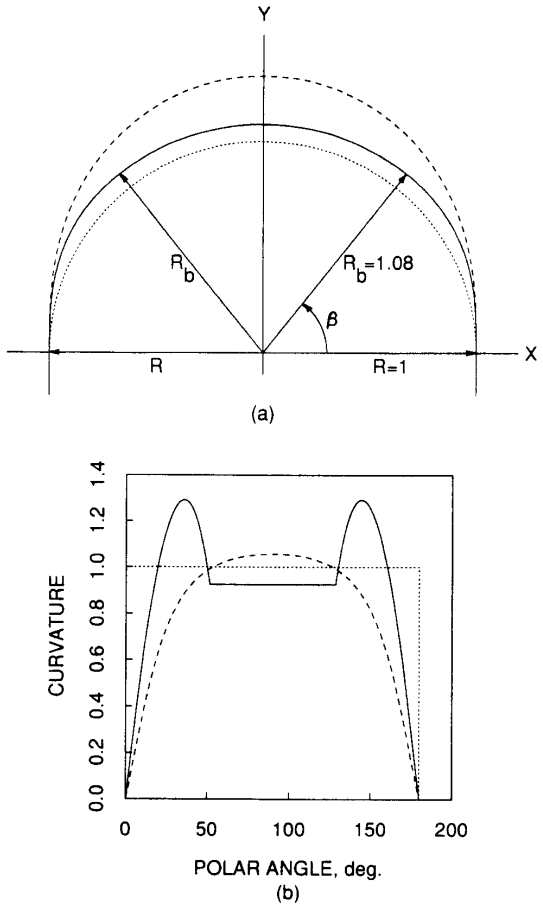

Fig. 4. (a) A 180-degree arc turn using a polar spline (solid curve) with R=1, R_b=1.08, and β=0.9 radians. Also shown are an SPP curve (dashed), and a circular arc (dotted). (b) Curvature functions for the curves in (a).

2.2 Lane Change Maneuvers

Curves which produce a transition between parallel lanes in the same direction will be called lane-change maneuvers. The "lazy-S" type curves needed for such maneuvers are typically constructed out of two arc segments or an arc-line-arc sequence. These multiple segment paths can be replaced by a single cartesian-polynomial segment that provides a continuous-curvature transition between the parallel lanes of travel.

A quintic polynomial, y(x), can be written as

$$y(x) = a_0+a_1x+a_2x^2+a_3x^3+a_4x^4+a_5x^5 \quad . \qquad (12)$$

Consider the lane-change maneuver in the coordinate frame shown in Figure 5(a). The six coefficients in (12) are chosen to satisfy the position, slope, and curvature constraints of this maneuver, namely,

$$\begin{aligned} &y=0\ , \quad \frac{dy}{dx}=0\ , \quad \kappa=0 \quad \text{at } x=0 \quad , \\ &y=y_e\ , \quad \frac{dy}{dx}=0\ , \quad \kappa=0 \quad \text{at } x=x_e \quad , \end{aligned} \qquad (13)$$

where κ is the curvature of $y(x)$, given by

$$\kappa = (d^2y/dx^2)/[1 + (dy/dx)^2]^{3/2} \quad .$$

The single cartesian-polynomial (SCP) curve satisfying the constraints (13) has only three non-zero coefficients, and can be written in the form

$$y(x) = y_e\left[10\left(\frac{x}{x_e}\right)^3 - 15\left(\frac{x}{x_e}\right)^4 + 6\left(\frac{x}{x_e}\right)^5\right] \qquad (14)$$

The SCP curve resulting from (14) is shown in Figure 5(a). The curvature, κ, as a function of x, shown in Figure 5(b), confirms that the SCP curve provides the desired continuous-curvature path. The maximum curvature and curvature-rate for the function shown in Figure 5(b) increase directly with the lane-change slope ratio, y_e/x_e. This ratio must be chosen sufficiently low so that the resulting continuous steering-function does not violate the peak steering and steering-rate constraints for a particular AGV design. Given that these constraints are met, the simple three-term expression (14) for the SCP curve applies to lane-change segments of arbitrary location and orientation in the workspace layout by transforming from the coordinate frame shown in Figure 5(a) to the coordinate frame aligned with the lane-change starting point. Although not providing the near-optimal smoothness of an arc-arc or arc-line-arc sequence using SPP curves, the SCP curve does provide a smooth, continuous-curvature lane change using only a single segment.

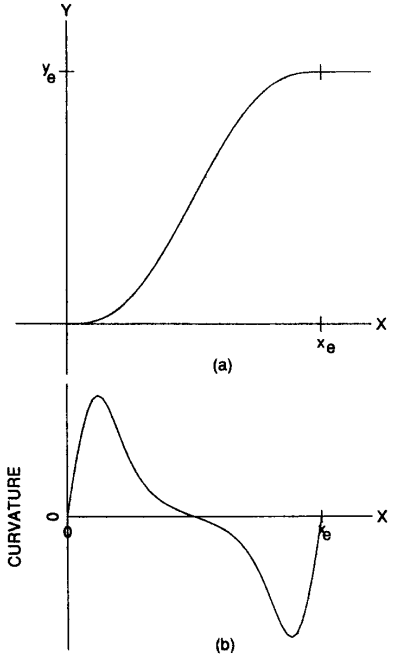

Fig. 5. (a) Lane-change maneuver from a single cartesian polynomial(SCP), (b) Curvature function of the SCP segment.

3. CONCLUSION

When a skilled car-driver makes a turn, the steering-wheel angle is smoothly increased to some maximum angle, then smoothly reduced back to the neutral position as the car comes out of the turn. It seems reasonable that paths generated for an autonomously guided vehicle should likewise have turn segments which permit such smooth steering commands for guiding the vehicle around turns in the path. If the generation of such smooth curves requires numerical integration of a curvature function along the curve length, with precise matching of position and heading conditions at the start and end points, it may be preferable to stay with circular arcs, and rely on the feedback control mechanism on the AGV to eventually remove the tracking errors.

If, however, the smooth curves can be generated as explicit functions that match the boundary conditions exactly, and are not much more complicated to generate than circular arcs, then they become more attractive to use for generating AGV paths. Two such types of curves have been described in this paper: single polar-polynomial (SPP) or polar spline curves for arc turns, and single cartesian-polynomial (SCP) curves for lane changes. They provide continuous curvature transitions across the line-curve junctions, and are reasonably simple polynomial functions with coefficients determined explicitly by the end-point parameters. The SPP curves have the further advantage of providing near-optimally smooth paths (see Appendix), and are generally preferable to multi-segment polar splines, except for large-angle (>90 deg.) arc turns on paths where it is important for the curves to remain close to circular arcs.

The SPP and SCP curves described above have been used in both the simulation and the actual path control system for an experimental tricycle-type cart[10]. The change from circular arcs to these continuous-curvature segments has significantly reduced both the magnitude and extent of the transient errors at line-arc-line transitions on the path, particularly at speeds greater than 10 in/s. Shown in Figure 6 are two examples, using the simulation program[10], of the experimental cart's performance in following a 90-degree, 35-inch radius turn at a speed of 12 in/s. The conditions for the two runs are the same, except that the turn segment in the left path is a circular arc, while in the right path it is an SPP curve. The peak tracking error in following the path with the circular arc is about 6 times the error in following the one with the SPP curve, and the transient persists much further along the line segment after the circular arc turn.

The change in the reference-path-generator code, needed to generate continuous-curvature SPP and SCP path-segments instead of circular-arc path-segments, produced no significant increase in the real-time computational load for the onboard computer. Since the use of continuous-curvature paths eliminates steering-function discontinuities in differential-drive as well as steered-wheel

vehicles[3],[6], and since the continuous-curvature path-segments described above are simple to generate, it can therefore be concluded that their use provides a worthwhile means for improving AGV path-tracking performance.

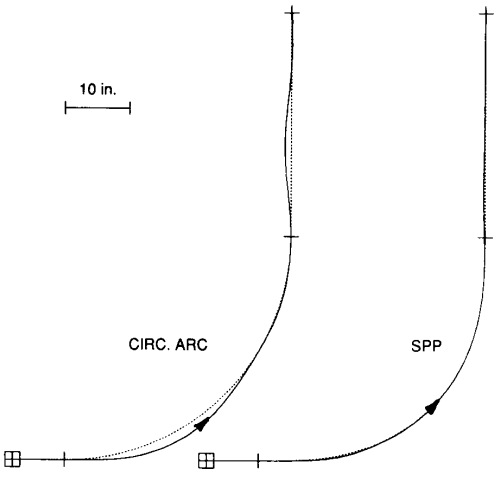

Fig. 6. Path tracking data for experimental AGV following paths with 90-degree turns at 12 in./s. The turn segment in the left path is a circular arc, while that in the right is an SPP segment. The AGV paths are the solid lines; the reference paths are the dotted lines.

APPENDIX: Patterns of Motion

Within the straight-line (linear) segments of a path, many of the physical constraints on the motion can be described in terms of the velocity-time pattern[11]. For example, to move between stops along a linear path under peak-acceleration constraints, the minimum-time performance is represented by a velocity-time profile that is *triangular* in shape, with sides having slopes equal to the peak acceleration and deceleration, and with an area under the curve equal to the distance moved. If the height of this velocity-time triangle violates the speed limit for the vehicle, the minimum-time performance has a *trapezoidal* velocity pattern with an area equal to the distance, a height equal to the speed limit, and sides with slopes corresponding to the acceleration/deceleration constraints. If minimum-integral-square acceleration (min-ISA) rather than minimum-time is the primary concern, it can be shown that the velocity pattern should be *parabolic* in shape[11].

Within the curve segments of the path, the physical constraints on the curved motion can be described in an analogous manner using the curvature-length pattern instead of the velocity-time pattern, where the curvature, κ, is defined by Eq. (3) of Sec. 2.1 above. From the definition of arc turns in Sec. 2.1 it follows that the *area* under the curvature-length pattern of an arc turn is equal to the *turn angle*. These relationships are illustrated in Figure A-1, which shows the curvature patterns of three curves having the same turn angle, Θ, and the same peak curvature, K_p. The rectangular pattern is the curvature pattern of a circular arc of radius, $1/K_p$. The base of the rectangle is the *length* of the circular arc, Θ/K_p. This length is marked L_{min} in Figure A-1, since there obviously can be no other pattern having the same area (turn angle) and height (peak curvature) with a shorter base (length).

For a vehicle moving on a curve at constant speed, V, the only acceleration is the centripetal acceleration, given by $a_c=V^2\kappa$. The *jerk*, which is the time derivative of the acceleration, is given by

$$j_c = V^2 d\kappa/dt = V^3\kappa' \quad ,$$

where $\kappa' \equiv d\kappa/ds$. The jerk is therefore proportional to the *slope* of the curvature pattern. By direct analogy with the minimum-time velocity patterns for linear motion[11], the minimum-length continuous-curvature path for a given turn angle, constrained only by the peak jerk, J_p, has a *triangular* curvature pattern with sides having slopes equal to $\pm J_p/V^3$, and with an area under the triangle equal to the turn angle. Since the clothoid pair[6] has this triangular curvature pattern, it corresponds to the minimum-length curve under a peak-jerk constraint. However, if the height of this triangle exceeds the curvature limit, K_p, for the vehicle, then it is apparent from the curvature pattern that the minimum-length curve must have a *trapezoidal* curvature pattern with an area equal to the length, a height equal to the curvature limit, and sides with slopes corresponding to the peak jerk constraint. This curve, which could be called a "clothoid-arc-clothoid", has the dashed line curvature pattern shown in Figure A-1.

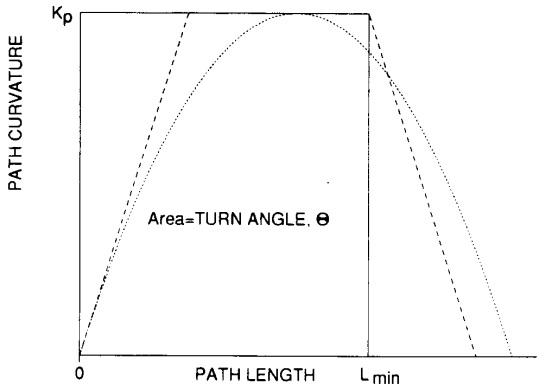

Fig. A-1. Curvature patterns for three curves having the same turn angle, Θ, and peak curvature, K_p. The *area* under each curve is Θ.

Since the min-ISA linear motion, described above, has a parabolic-shaped velocity pattern, we can predict by analogy that the minimum integral-square-jerk(ISJ) arc turn should have a parabolic-shaped curvature pattern. Kanayama and Hartman's optimally smooth "cubic spiral"[7] corresponds to a min-ISJ curve, and indeed, they show that it has a curvature function that is *parabolic* in shape. This optimally smooth curve has the dotted-line curvature pattern shown in Figure A-1. From this figure it is obvious that, for the same peak-curvature(height) and peak-jerk(slope) constraints, the cubic spiral must have a greater length(base) than the clothoid-arc-clothoid curve. The curvature pattern for any curved path can be used in this manner to show how well it meets various objectives and constraints of the motion.

REFERENCES

1. J. M. Hollerbach, "Dynamic scaling of manipulator trajectories," *J. of Dyn. Sys. Meas. and Control*, **106**, pp. 102-106, 1984.
2. T. J. Graettinger and B. H. Krogh, "Evaluation and time-scaling of trajectories for wheeled mobile robots," *Proc. American Control Conf.*, Atlanta, GA, June 1988.
3. W. L. Nelson, "Continuous steering-function control of robot carts," to be publ. in *IEEE Trans on Industrial Electronics*, 1989.
4. L. E. Dubins, "On curves of minimal length with a constraint on average curvature, and with prescribed initial and terminal positions and tangents," *American Journal of Mathematics*, **79**, pp. 497-516, 1957.
5. R. C. Yates, *Curves and Properties*, Classics Publishing Co., 1952.
6. Y. Kanayama and N. Miyake, "Trajectory generation for mobile robots," *Proc. 3rd Int'l Symp. on Robotics Research*, O. D. Faugeras and G. Giralt, eds., Gouvieux, France, pp. 333-340, 1985.
7. Y. Kanayama and B. Hartman, "Smooth local path planning for autonomous vehicles," Univ. of California, Santa Barbara, Tech. Report TRCS88-15,1988.
8. W. L. Nelson, "Continuous-curvature paths using quintic and polar polynomials," AT&T Bell Labs internal document, Mar. 30, 1988.
9. C. be Boor, *A Practical Guide to Splines*, Springer-Verlag, 1978.
10. W. L. Nelson and I. J. Cox, "Local path control for an autonomous vehicle," *Proc. 1988 IEEE Int'l Conf. on Robotics & Automation*, Philadelphia, PA, April 24-29, 1988.
11. W. L. Nelson, "Physical principles for economies of skilled movements," *Biological Cybernetics*, **46**, pp. 135-147, 1983.